

Software and Hardware System for the Investigation of the Thin Film Optical Properties

M.G. Demydenko, S.I. Protsenko*, K.V. Tyschenko, O.V. Fedchenko

Sumy State University, 2, Rimsky Korsakov Str., 40007 Sumy, Ukraine

(Received 12 April 2012; in final form 23 May 2012; published online 04 June 2012)

Using the Thorlabs optical elements and graphic software development system LabVIEW 2010, the software and hardware automated system for the investigation of the optical properties of multilayer film systems was developed. The joint genetic algorithm was proposed to process the experimental data of the null ellipsometry and the X-ray reflectometry. It was shown that the given technique lets one simulate phase transitions, diffusion processes, and interface blurring in multilayer film systems very accurate for different computational theoretic models.

Keywords: Null ellipsometry, X-Ray reflectometry, Optical coefficients, Frenel equations, Genetic algorithm.

PACS numbers: 07.60.Fs, 06.05.cm

1. INTRODUCTION

While investigating the electrophysical and magnetoresistive properties of thin films and spin-valve systems, it is important to know the features of diffusion processes, possibility of conservation of individuality of the film system separate layers, and about solid-phase reactions occurring in such systems during condensation and further thermal treatment.

The X-ray reflectometry method is often used in the study of the degree of individuality of separate layers and diffusion processes in multilayer film systems. But while investigating spin-valve systems based on Co/Cu multilayers, a number of difficulties appear which are connected with the fact that density of Co and Cu layers and optical constants of substances in the X-ray range are very close, and, therefore, it is very difficult to distinguish them experimentally. In connection with this, the main aim of the present work was to organize the complete closed cycle of investigation of multilayer film systems using combination of the standard small-angle X-ray diffractometer and the null ellipsometer which we have been proposed [1, 2].

Using the null ellipsometry method during investigation of nanosized spin-valve systems based on multilayer Co/Cu films, one can obtain the exact values (in contrast to the X-ray reflectometry method) of optical parameters of the refraction coefficients n and k , since they have different absolute values. Therefore, combination of the small-angle X-ray diffraction and the null ellipsometry methods gives the possibility to study more precisely the peculiarities of the diffusion and phase-formation processes in multilayer nanosized Co/Cu films as the components of spin-valve systems.

For realization of the above mentioned closed cycle of investigations, we have used the series small-angle diffractometer Bruker D8 Discover and the developed software and hardware system for the investigation and analysis of the optical properties of multilayer films by the null ellipsometry method.

2. SOFTWARE AND HARDWARE COMPLEX OF AUTOMATED NULL ELLIPSO METER

* serhiy.protsenko@gmail.com

When producing the null ellipsometer we have used the Thorlabs optical elements (analyzer, polarizer, and compensator) with possibility of program control using step motors, laser with the wavelength of $\lambda = 6328 \text{ \AA}$, and arms with the constant incident and reflection angle of 70° of the laser beam from the sample.

In Fig. 1 we represent the appearance and optical scheme of the developed null ellipsometer.

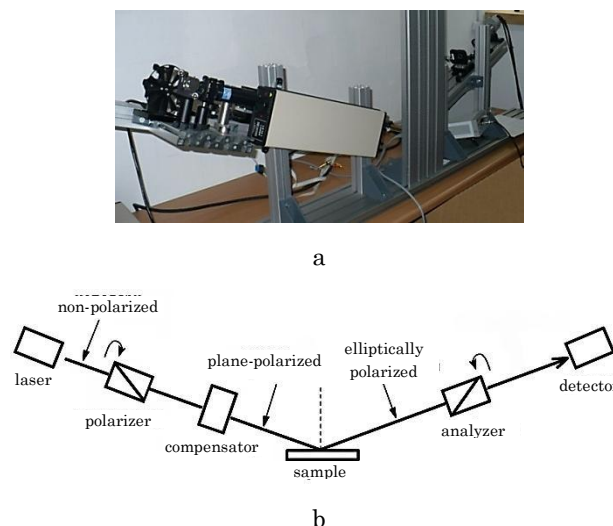


Fig. 1 – External view of the null ellipsometer (a) and its optical scheme (b)

When developing the software and hardware complex of the null ellipsometer, we have used a classical scheme which is based on the automated rotation of polarizer and analyzer [3] and involves the modulated light source with collinear optics, polarizer, compensator, analyzer, focusing optics, detector (photoelectric multiplier), signal from which goes on the Lock-in amplifier where after treatment is given through the GPIB interface to the control software on PC.

In Fig. 2 we show the external view of the software in the search mode of the experimental values Δ and ψ (ellipsometric angles) by four zones.

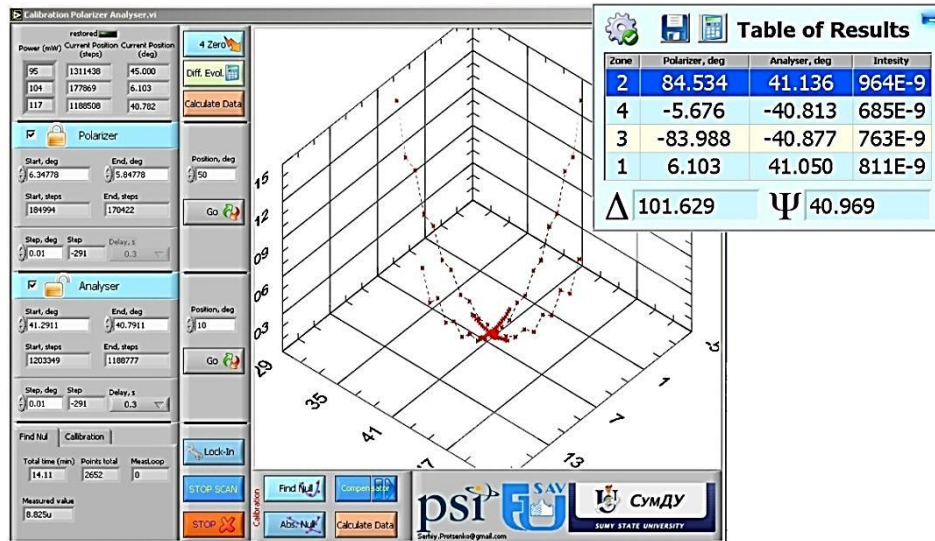


Fig. 2 – External view of the developed software for the control of null ellipsometer in the search mode of Δ and ψ values in four zones

In this null ellipsometer mode, compensator is fixed on the level of $1/4$ of the wavelength $\delta = 90^\circ$ with deflection of $\pm 45^\circ$. Due to the iterative cyclic change in the polarizer control angle (at the fixed value of compensator angle) and at the iterative change in the analyzer control angle (at the fixed values of compensator and polarizer angles), it is possible to achieve the pairs of angle values of polarizer and analyzer at which linearly polarized light can be completely quenched. As a result, the values of polarizer and analyzer angles, at which almost zero signal is observed on detector, are equal to ellipsometric angles Δ and ψ . To increase the accuracy of the obtained results, Δ and ψ values were averaged by zero search in the so-called four zones at the change in the polarizer and analyzer angles from 0 to 90° (at two values of the compensator angle of $\pm 45^\circ$) and change in the polarizer and analyzer angles from 0 to 90° (at two values of the compensator angle of $\pm 45^\circ$).

Software for the control of all subsystems of the null ellipsometer was realized using the development system LabVIEW 2010, since usage of just such software, but not hardware, approach allows to flexibly change the operation modes of the device and apply different control schemes depending on the type of the studied samples.

In Fig. 3 we illustrate the comparative experimental results of the values of Δ and ψ parameters for SiO_2/Si system obtained on the null ellipsometer which we had developed and on the series device of the University of Technology in Bratislava (Slovakia). As seen from the figure, coincidence is considered to be acceptable, and insignificant differences can be explained by oxide non-uniformities on the substrate surface and different measurement conditions.

Since simple analytical correlation between ellipsometric angles Δ and ψ and optical reflection (n) and refraction (k) coefficients does not exist, then in order to find the values of n and k as well as the thickness of separate layers (d_i) in multilayer film systems it is necessary to solve the inverse ellipsometry problem.

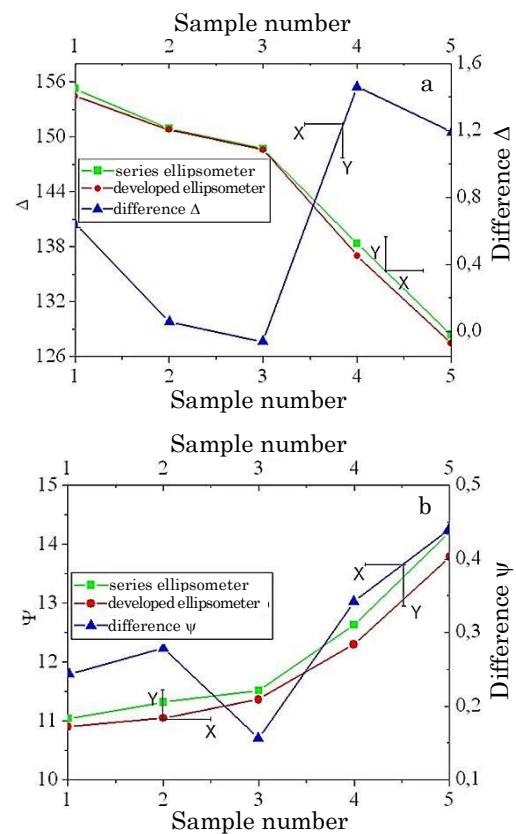


Fig. 3 – Comparison of the experimental parameters Δ and ψ for SiO_2/Si system obtained on the developed null ellipsometer and series device

But we have to note that during determination of the absolute values of d_i , n , and k , a number of possible solutions considerably increases with the increase in the number of layers of film structure. We have used the genetic algorithm (GA) method [4, 5] in order to find just the physical values of the optical reflection (n) and refraction (k) coefficients and the thickness of separate layers (d_i).

3. CALCULATION MODELS FOR THE ANALYSIS OF THE EXPERIMENTAL DATA OF THE X-RAY REFLECTOMETRY AND ELLIPSOMETRY OF FILM SYSTEMS USING GENETIC ALGORITHM

The main aim of the present part of the work was to develop the software for determination of the optical characteristics, roughness of the interfaces, and thickness for each layer of multilayer system. The specified problem was solved using compatible genetic algorithm which combines the analysis of the experimental data of the null ellipsometry and X-ray reflectometry. Different models were used for the calculations: Parratt, Gibaud, profile, interdiffusion, replication models and the model which takes into account the presence of intermediate layer [6-9]. The usage of these models allows to approach to the real system parameters in order to increase the analysis accuracy of the experimental results. While solving the inverse ellipsometry and X-ray reflectometry problem, it is necessary to simultaneously find a large amount of unknown variables using some experimental values, therefore, usage of the genetic algorithms is reasonable. In comparison with usual optimization methods they have the following features: parallel search, random mutations, and recombinations of the already obtained solutions. GA is well suited as a simple heuristic optimization method of multidimensional badly defined functions.

The software was developed in the graphical programming environment LabVIEW 2010 of the company National Instruments. It has the advantage at creation of parallel software with a large amount of simultaneously operating flows, since it represents two-dimensional programming language with support for native parallelism.

The external view of the faceplate of the developed software is illustrated in Fig. 4.

When working with the application, there is the possibility to specify the layer material, its optical

parameters n and k , layer thickness d , search limits $n_{\min} - n_{\max}$, $k_{\min} - k_{\max}$, and $d_{\min} - d_{\max}$. Additionally, using the setup control panel, user can determine the following parameters: incidence angle, wavelength, population size, strategy of genetic algorithm (there is the possibility of choice from 10 different strategies), cross-over, weighting, and choose formula for the calculation of the accuracy function.

The developed software has some interfaces which appear depending on the fact which model is chosen by user. The Parratt model [6] is the basic one for the solution of the inverse ellipsometry problem and for calculation of the theoretical reflectometry. In this model, the dependence between the optical layer constants and parameters of elliptically polarized light is established on the basis of the Fresnel correlations

$$r_j = \frac{k_{zj} - k_{zi}}{k_{zj} + k_{zi}} \exp \left[-2(k_{zj} \cdot k_{zi})^{1/2} \sigma_j \right], \quad (1)$$

where r_j is the Fresnel coefficient for reflection from the surface between i -th and j -th layers; k is the perpendicular component of the wave vector in j -th or i -th layer; σ is the RMS, the value which takes into account the surface roughness.

$$k_j = \frac{2\pi}{\lambda} n_j \cos \theta_j, \quad (2)$$

where λ is the wavelength; n_j is the complex reflection index; θ_j is the wave incidence angle on the plane (it is defined for all system layers using the optics laws).

Complex reflection coefficient $n = n + ik$ (where n is the reflection coefficient and k is the wave attenuation coefficient) is determined for two neighbor layers n_i , n_j . Amplitudes of the electric fields which penetrated and were reflected are defined from the Fresnel correlations for s - and p -polarization

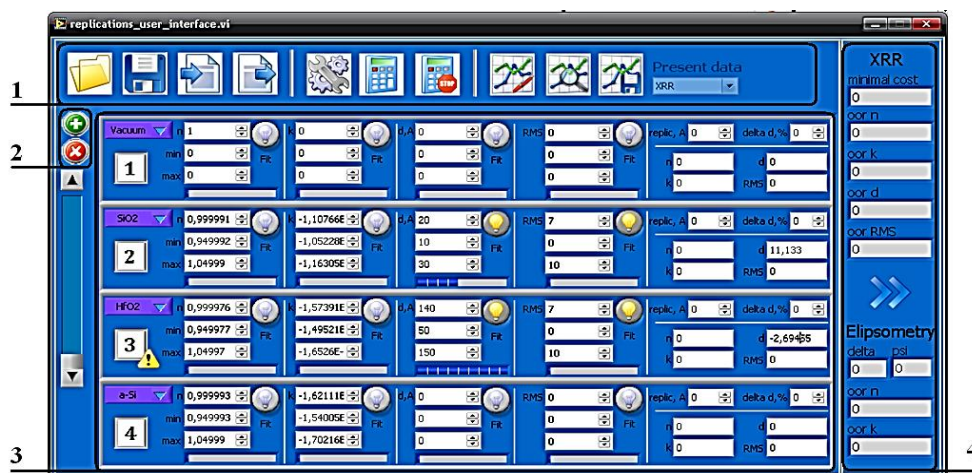


Fig. 4 – External view of the faceplate of the developed software: 1 – group of buttons which is used for operations with files, for calculation settings, start, and shut-down, and dealing with graphs; 2 – buttons which are used for layer addition or removal in the calculation stack; 3 – array of clusters which is intended to specify the calculation stack; 4 – region which indicates current values of the calculation accuracy for the reflectometry and ellipsometry, and the data of ψ and Δ

$$r_{ij}^S = \frac{n_i \cos \theta_i - n_j \cos \theta_j}{n_i \cos \theta_i + n_j \cos \theta_j} \cdot \exp \left[-2 \left(\frac{4\pi^2}{\lambda^2} n_j n_i \cos \theta_j \cos \theta_i \right)^{1/2} \sigma_j \right], \quad (3)$$

$$r_{ij}^P = \frac{n_i \cos \theta_j - n_j \cos \theta_i}{n_i \cos \theta_j + n_j \cos \theta_i} \cdot \exp \left[-2 \left(\frac{4\pi^2}{\lambda^2} n_i n_j \cos \theta_i \cos \theta_j \right)^{1/2} \sigma_j \right], \quad (4)$$

where n is the complex reflection coefficient; $\theta_{j,i}$ is the wave incidence angle on j -th or i -th layer; σ_j is the RMS of j -th layer.

Based on the correlations (3)-(4), general reflection coefficients are determined with taking into account the complex component φ_j of the wave scattering coefficient in the layer thickness d_j

$$r_p = \frac{r_{ij}^p + r_{p+1} \cdot \varphi^2}{1 + r_{p+1} \cdot r_{ij}^p \cdot \varphi^2}, \quad (5)$$

$$r_s = \frac{r_{ij}^s + r_{s+1} \cdot \varphi^2}{1 + r_{s+1} \cdot r_{ij}^s \cdot \varphi^2}, \quad (6)$$

where $\varphi_j = \exp(ik_j d_j)$.

Azimuth and phase difference (Ψ and Δ) are defined using the known values of r_p and r_s

$$\Psi = \text{Re} \left(\frac{r_p}{r_s} \right) \cdot \frac{180}{\pi}, \quad (7)$$

$$\Delta = \text{Im} \left(\frac{r_p}{r_s} \right) \cdot \frac{180}{\pi}. \quad (8)$$

When calculating the theoretical reflectometry based on the Parratt model, after general reflection coefficient for p -polarization, the reflectometry coefficient R (the reflectance) is determined: $R = |r_p|^2$.

Since real surfaces have non-ideal morphology (roughness), it is necessary to use additional model in the software which allows to take into account the geometry of these non-uniformities on the layer surface. Depending on the morphology type, calculations are performed by different formulas. Disadvantage of this model is the fact that it describes surface irregularities with a certain approximation.

In real multilayer systems have place both the non-uniformities and their replications from layer to layer, therefore, the replication model is also provided in the developed software. It allows to specify the results of the Parratt model using the RMS coefficients and reflection of non-uniformities of the first layer to the following.

Using the X-ray reflectometry or null ellipsometry and the Fresnel coefficients, one can calculate the thicknesses and optical characteristics of the diffusion boundary, i.e. intermediate layers which appear due to the diffusion between layers of different materials. In the developed software, such calculations are carried out using the "graded" model. Intermediate layer is characterized by three parameters: thickness of the diffusion boundary w_g ; a number of layers in this boundary N_g , distribution factor X_g which determines where the intermediate layer is located with respect to the initial interface (before diffusion) (see Fig. 5).

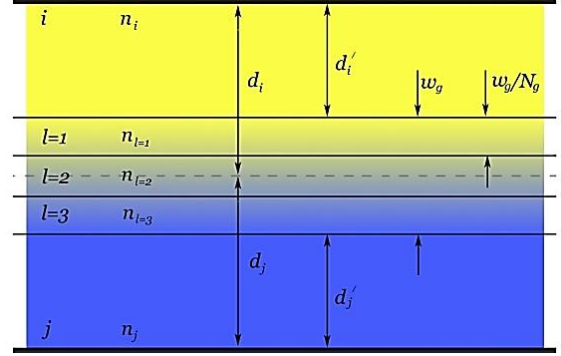


Fig. 5 – Model of multilayer system with intermediate layers which appeared due to the diffusion

The thickness of each of N_g layers is equivalent to w_g/N_g , and the optical characteristics of each l -th layer ($l = 1, 2, \dots, N_g$) are calculated by the following relation:

$$n_l = \frac{(N_g + 1 - l)n_i + l n_j}{(N_g + 1)}, \quad (9)$$

$$k_l = \frac{(N_g + 1 - l)k_i + l k_j}{(N_g + 1)}. \quad (10)$$

The resulting layer thickness of pure material d_i' and d_j' after taking into account the presence of the diffusion region is defined as

$$d_i' = d_i - w_g(1 - X_g), \quad (11)$$

$$d_j' = d_j - w_g X_g. \quad (12)$$

The given model allows to determine the basic parameters of the diffusion region [9].

4. RESULTS AND DISCUSSION

Calculated and plotted due to the developed software graphs of the reflectometry were compared with the experimental and theoretical ones obtained by the GenX (this is the universal program which is used to obtain the X-ray and neutron reflectometry data) [10].

In Fig. 6 we illustrate the comparison of the experimental graph with the theoretical one plotted using the developed software for $\text{HfO}_2(14 \text{ nm})/\text{SiO}_2(2 \text{ nm})/\text{a-Si}$ multilayer system.

In Fig. 7 we show the results of GenX work: the red line is the experimental reflectometry; the blue line is the theoretical calculations of GenX for the system $\text{Fe}(1,1 \text{ nm})/\text{Pt}(1,6 \text{ nm})_{24}\text{Pt}(4,5 \text{ nm})/\text{Fe}(1,1 \text{ nm})/\text{MgO}$ by the Parratt model.

In Fig. 8 we represent the comparison of the theoretical calculations of GenX (the green graph) and the developed software (the red graph) for the same system.

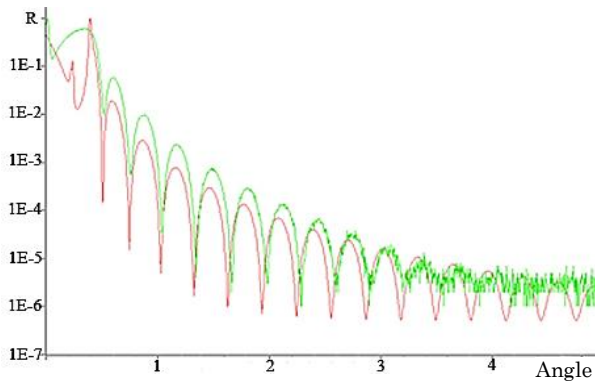


Fig. 6 – Comparison of the experimental (the green line) and calculated (the red line) dependences. The latter is obtained for $\text{HfO}_2(14 \text{ nm})/\text{SiO}_2(2 \text{ nm})/\text{a-Si}$ system using the developed software

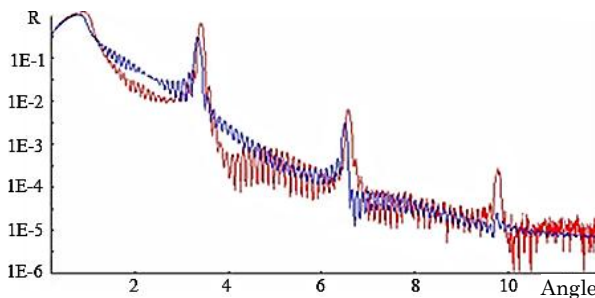


Fig. 7 – Comparison of the experimental and theoretical reflectometry (which is obtained as a result of the GenX work) for $(\text{Fe}(1.1 \text{ nm})/\text{Pt}(1.6 \text{ nm}))_{24}\text{Pt}(4.5 \text{ nm})/\text{Fe}(1.1 \text{ nm})/\text{MgO}$ system. The Parratt model was applied for the calculations

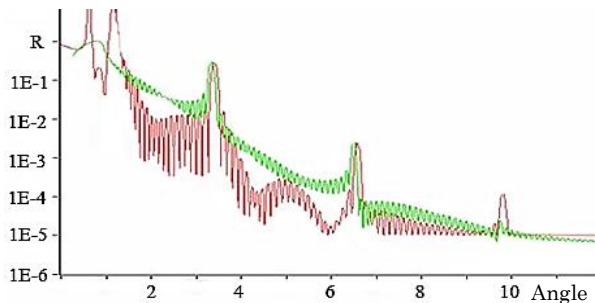


Fig. 8 – Comparison of the theoretical calculations of GenX (the green graph) and the developed software (the red graph) for the same system

As seen from these figures, for the Parratt model the developed software calculates reflectometry slightly better than GenX does.

REFERENCES

1. M. Björck, G. Andersson, *A short manual for GenX*, <http://genx.prog.googlepages.com/manuals>.
2. P.T. Patsalas, S. Logothetidis, P.C. Kelires, *Diam. Relat. Mater.* **14**, 1241 (2005).
3. H.G. Tompkins, E.A. Irene, *Handbook of ellipsometry* (Springer: 2005).
4. M.G. Demydenko, S.I. Protsenko, O.B. Protsenko, O.V. Fedchenko, *Visnyk SumDU. Seriya: Fizyka, matematyka, mekhanika* **1**, 33 (2008).

The profile model (exponential profile) was used for the calculations.

In Fig. 9 we show the calculations of the developed software for the model with intermediate layers (the graded model). It is seen as the X-ray reflectometry is changed in the presence of the diffusion processes.

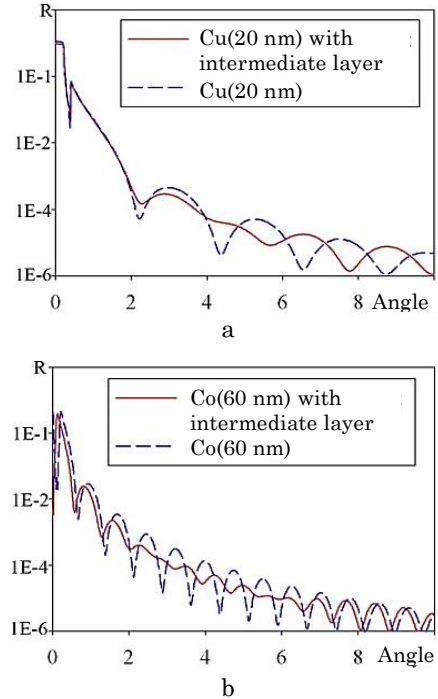


Fig. 9 – Calculations of the X-ray reflectometry (graded model) for Cu(20 nm) (a) and Co(60 nm) (b) films

5. CONCLUSIONS

Thus, different calculation models in the developed software allow to maximally approach the multilayer system to the real one due to the consideration of non-uniformities of the interfaces, replication, interdiffusion, and presence of intermediate layers. Usage of simultaneous treatment of the experimental data of the X-ray reflectometry and null ellipsometry allows to considerably decrease the measurement accuracy of the thickness and optical characteristics of layers. The genetic algorithm was used as the calculation method, since it operates well with a large amount of variables, does not get to the local minimum, and finds physical solutions.

5. M. Demydenko, S. Protsenko, P. Siffalovic, *Thin Solid Films* **520** (2012) (*In Press*).
6. L. Parratt, *Phys. Rev.* **95**, 359 (1954).
7. D.L. Windt, *Comput Phys.* **12**, 360 (1998).
8. I. Pape, T.P.A. Hase, B.K. Tanner, M. Wormington, *Physica B* **253**, 278 (1998).
9. A. Gibaud, S. Hazra, *Current Science* **78**, 1467 (2000).
10. M. Björck, G. Andersson, *J. Appl. Cryst.* **40**, 1174 (2007).